ACCOUNTS of chemical research

Article

pubs.acs.org/accounts

Switchable Reconfiguration of Nucleic Acid Nanostructures by Stimuli-Responsive DNA Machines

Xiaoqing Liu,‡ Chun-Hua Lu,‡ and Itamar Willner*

Institute of Chemistry, Center for Nanoscience and Nanotechnology, The Hebrew University of Jerusalem, Jerusalem 91904, Israel

CONSPECTUS: The base sequence in DNA dictates structural and reactivity features of the biopolymer. These properties are implemented to use DNA as a unique material for developing the area of DNA nanotechnology. The design of DNA machines represents a rapidly developing research field in the area of DNA nanotechnology. The present Account discusses the switchable reconfiguration of nucleic acid nanostructures by stimuli-responsive DNA machines, and it highlights potential applications and future perspectives of the area.

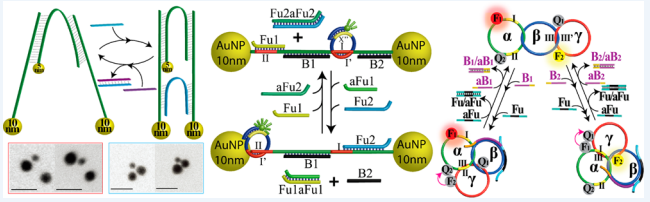

Programmed switchable DNA machines driven by various fuels and antifuels, such as pH, Hg^{2+} ions/cysteine, or nucleic acid strands/antistrands, are described. These include the assembly of DNA tweezers, walkers, a rotor, a pendulum, and more. Using a pH-oscillatory system, the oscillatory mechanical operation of a DNA pendulum is presented. Specifically, the synthesis and "mechanical" properties of interlocked DNA rings are described. This is exemplified with the preparation of interlocked DNA catenanes and a DNA rotaxane. The dynamic fuel-driven reconfiguration of the catenane/rotaxane structures is followed by fluorescence spectroscopy. The use of DNA machines as functional scaffolds to reconfigurate Au nanoparticle assemblies and to switch the fluorescence features within fluorophore/Au nanoparticle conjugates between quenching and surface-enhanced fluorescence states are addressed. Specifically, the fluorescence features of the different DNA machines are characterized as a function of the spatial separation between the fluorophore and Au nanoparticles. The experimental results are supported by theoretical calculations.

The future development of reconfigurable stimuli-responsive DNA machines involves fundamental challenges, such as the synthesis of molecular devices exhibiting enhanced complexities, the introduction of new fuels and antifuels, and the integration of new payloads being reconfigured by the molecular devices, such as enzymes or catalytic nanoparticles. Exciting applications of these systems are ahead of us, and switchable catalytic nanoparticle systems, switchable enzyme cascades, and spatially programmed nanoparticles for innovative nanomedicine may be envisaged. Also, the intracellular reconfiguration of nucleic acids by stimuli-responsive DNA machines holds great promise as a means to silence genes or inhibit metabolic pathways.

INTRODUCTION

The base sequence in DNA encodes substantial structural and functional information into the biopolymer. The reactivity of the biopolymer in the presence of enzymes, such as endonucleases or nicking enzymes, the sequence-specific recognition by nucleic acids (aptamers) toward low-molecular-weight substrates,[1] macromolecules, and even cells, the specific interactions of nucleic acids with proteins, and the sequence-dictated catalytic functions of nucleic acids (DNAzymes or ribozymes) are controlled by the DNA structures.[2] These unique features of nucleic acids make DNA an attractive functional material for the development of DNA nanotechnology.[3] Different research topics have been addressed within the broad scope of DNA nanotechnology, including the ingenious self-assembly of 1D, 2D, and 3D DNA nanostructures,[4] the organization of DNA/nanoparticle[5] and DNA/protein hybrid nanostructures,[6] the fabrication of supramolecular sensing platforms,[7] the use of nucleic acids as functional materials for computing,[8] and the use of DNA as a template for the construction of nanoscale devices.[9]

The development of DNA machines represents an active research topic in the area of DNA nanotechnology.[10] A DNA machine is a supramolecular nucleic acid structure that performs, in the presence of the appropriate triggers, macroscopic machinelike functions. Such DNA machines have promising future applications as biomedical and environmental sensing devices and in monitoring of intracellular metabolic pathways, nanomedicine, switchable plasmonics, and more. DNA machines are characterized by several fundamental features: (i) The DNA machine is triggered by an external fuel. The machine may reveal autonomous operation until the full consumption of the fuel, or it may reveal programmed transitions across predefined states. (ii) The transitions of the machine are energetically downhill ($\Delta G < 0$). (iii) The operation of the DNA machine may consume the fuel, and the process might yield a "waste" product. (iv) The DNA machine might exhibit unidirectional operation or reversible cyclic operation. In the case of reversible DNA machines, the

Special Issue: Nucleic Acid Nanotechnology

Received: December 26, 2013
Published: March 21, 2014

   dx.doi.org/10.1021/ar400316h | Acc. Chem. Res. 2014, 47, 1673−1680

incorporation of an "antifuel" trigger that compensates for the "fuel" trigger is essential.

During the past decade, substantial progress in the area of DNA machines was accomplished, and several review articles have addressed the advances in the field.[11] In the present Account, we exemplify DNA machines developed by our laboratory and discuss these systems within the broad context of the field. Specifically, we aim to describe DNA machines driven by a chain of different fuels and antifuels and to highlight the switchable reconfiguration of nucleic acid structures and metal nanoparticle assemblies by DNA machines. Furthermore, plasmonic control of the fluorescence features of Au nanoparticle/fluorophore conjugates by means of DNA machines are discussed.

STIMULI-TRIGGERED DNA MACHINES

The thermodynamics associated with the formation of DNA duplexes[12] or DNA nanostructures such as the i-motif[13] or G-quadruplexes[14] has been widely applied as a driving force to operate DNA machines. The effects that stabilize duplex DNA structures include the number of base pairs, the nature of the bases,[12] and cooperative effects such as ion bridging (T−Hg^{2+}−T or C−Ag^{+}−C)[15] and intercalation of photoisomerizable units (e.g., *trans*-azobenzene).[16] Indeed, different DNA machines such as gears,[17] tweezers,[18] and walkers[19] or the reconfiguration of DNA structures by means of strand displacement,[18] pH,[20] ions,[21] and light[16] have been reported. In these systems, switchable transitions of the devices are controlled by the formation of duplexes with enhanced stabilities, in the presence of the appropriate fuels, and the subsequent dissociation of the structures upon addition of the respective antifuels. Although substantial progress in the development of fueled/antifueled DNA machines has been accomplished, several challenges still exist: (i) The development of DNA machines activated by a chain of different fuels and antifuels is an interesting path to follow. (ii) The assembly of DNA machines on surfaces introduces new concepts for the construction of nanoscale devices. Specifically, the activation of DNA machines or their imaging by electrical or photoelectrochemical stimuli might introduce innovative bioelectronic systems. (iii) The stimuli-responsive switchable reconfiguration of DNA nanostructures might be accompanied by the carriage of molecular (e.g., fluorophores), macromolecular (e.g., enzymes), or nanoparticle components. These might lead to the switchable control of plasmonic functions or catalytic features. The present Account will address recent developments accomplished by our laboratory in the area of stimuli-responsive DNA machines. Efforts will be directed to highlight the future perspectives of the topic.

The pH- and Hg^{2+}/cysteine-stimulated switchable activation of DNA tweezers[21,22] is depicted in Figure 1. The pH-triggered tweezers consisted of C-rich arms (**1**) and (**2**) that were bridged by nucleic acids (**3**) and (**4**) to yield the closed structure of the tweezers (Figure 1A). At pH 5.2 the arms form the i-motif structure, a process that releases (**4**) and results in the open structure of the tweezers. Neutralization of the system (pH 7.2) dissociates the i-motif structure, leading to the rebinding of (**4**) to the arms and closure of the tweezers. By labeling of the bridging unit (**3**) with a fluorophore/quencher pair, the switchable opening and closure of the tweezers was transduced by controlling the fluorescence intensity of the label (lower intensity → closed tweezers, higher intensity → open tweezers; Figure 1B). Similarly, the Hg^{2+}-ion-assisted cooperative bridging of nucleic acid arms (**5**) and (**6**) by nucleic acids (**7**) and (**8**) through the formation of T−Hg^{2+}−T complexes led to the formation of the closed tweezers (Figure 1C). Subjecting the closed tweezers to cysteine removed the Hg^{2+} ions by formation of the energetically stabilized Hg^{2+}−cysteine complex, resulting in the separation of the bridge (**8**) and opening of the tweezers. The switchable opening and closure of the tweezers was then followed by the fluorescence generated by the fluorophore/quencher pair (Figure 1D).

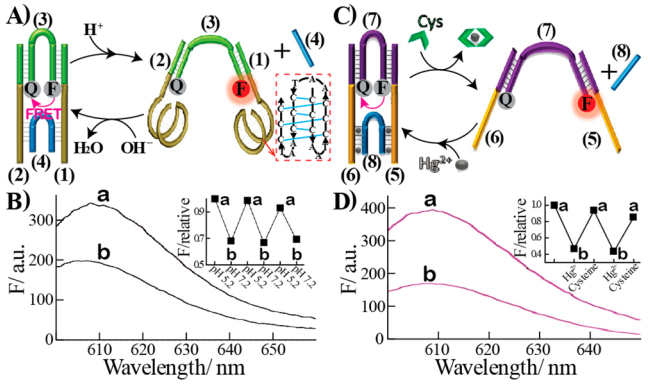

Figure 1. (A) pH-driven cyclic DNA tweezers. (B) Fluorescence spectra corresponding to (a) the open tweezers and (b) the closed tweezers. The inset shows cyclic fluorescence intensities: (a) the open tweezers at pH 5.2; (b) the closed tweezers at pH 7.2. (C) Cyclic Hg^{2+}/cysteine-stimulated closure and opening of DNA tweezers. (D) Fluorescence spectra corresponding to (a) the open tweezers and (b) the Hg^{2+}-assisted closed tweezers. The inset shows cyclic fluorescence intensities upon Hg^{2+}/cysteine-stimulated (a) opening and (b) closure of the tweezers. Reprinted with permission from refs 21 (copyright 2010 U.S. National Academy of Sciences) and 22 (copyright 2009 American Chemical Society).

A bidirectional, reversible, bipedal DNA walker driven by pH and Hg^{2+}/cysteine was constructed[23] (Figure 2A). A DNA scaffold composed of the five nucleic acids (**9**), (**10**), (**11**), (**12**), and (**13**) was constructed. The complementarity between the strands generated a stiff track with four footholds. Functional nucleic acids (**14**), (**15**), (**16**), and (**17**), each modified with a different fluorophore (F_1−F_4, respectively), were hybridized with the footholds, and each of these included a protruding single-stranded tether (I−IV, respectively) that provided the recognition sites for the bipedal walker. The "walker" element consisted of two units (**18**) and (**19**) that were bridged by the linker (**20**), which was modified at its 3′- and 5′-ends with black hole quencher units. The "walker" included two single-stranded "arms" that exhibited programmed complementarities with the recognition site. The primary, energetically stabilized structure of the walker involves its association to the recognition sites I and II, leading to quenching of the fluorophores F_1 and F_2 associated with these recognition sites. In the presence of Hg^{2+} ions as "fuel", the arm associated with site I is translocated to foothold III, where the resulting duplex is energetically stabilized by cooperative base pairing and T−Hg^{2+}−T bridges. In the resulting nanostructure, fluorophores F_2 and F_3 are quenched, while the fluorescence signals of F_1 and F_4 are triggered on (Figure 2B). The removal of the Hg^{2+} ions by the cysteine trigger induces the reverse transition of the "walker pedal" to site I. Under acidic conditions (pH 5.2), domain II folds into the i-motif structure, releasing the second "walker pedal" from site II. The free pedal then binds to the energetically less stable site IV, leading to

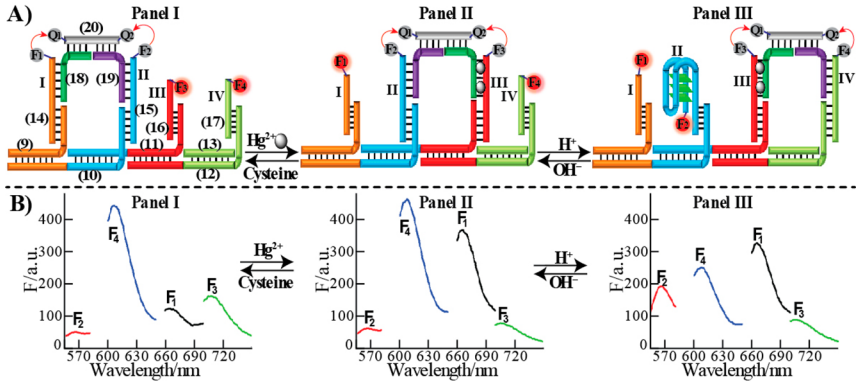

Figure 2. (A) A bidirectional bipedal walker on a DNA track consisting of four footholds. The walker is activated by H^+/OH^- and Hg^{2+}/cysteine as fuel/antifuel components. The "walking" process is read out by the quenched fluorescence signals of the fluorophores F_1−F_4 associated with the different footholds. (B) Panel I: the bipedal walker is positioned on footholds I and II (F_1 and F_2 quenched). Panel II: the bipedal walker is positioned on footholds II and III (F_2 and F_3 quenched). Panel III: the bipedal walker is positioned on footholds III and IV (F_3 and F_4 quenched). Reprinted with permission from ref 23. Copyright 2011 American Chemical Society.

quenching of fluorophores F_3 and F_4. Neutralization of the system (pH 7.0) separates the i-motif structures, resulting in the reverse transition of the walker pedal associated with site IV to the energetically favored binding site II.

DNA walker systems operating on surfaces represent a further advance in the design of DNA devices, particularly stimuli-switchable electrocatalytic and photoelectrochemical systems.[24] This is exemplified in Figure 3A by the construction of a two-state walker on an electrode, consisting of a track, (**21**), with which two protruding footholds, (**22**) and (**23**), were hybridized. The walker unit (**24**) includes a G-rich sequence, and its hybridization with foothold II yields an energetically stabilized duplex composed of a catalytically inactive ("caged") G-rich sequence. The fuel strand (**25**) displaces the walker, resulting in the translocation of the walker to the energetically less-favored site I, a process that uncages the G-rich sequence into a catalytically active hemin/G-quadruplex structure that stimulates the electrocatalyzed reduction of H_2O_2. By the removal of the fuel strand from foothold II, using the antifuel strand (**26**), the walker unit is separated from foothold I, and the reverse transition of the walker to site II occurs. This regenerates the catalytically inactive structure of the walker on foothold II. By reversible treatment of the nucleic acid-modified electrode with the fuel and antifuel strands, the cyclic ON−OFF electrocatalytic reduction of H_2O_2 by the hemin/G-quadruplex occurs, and the resulting cathodic currents transduce the position of the walker (Figure 3B). In a related DNA walker construct, the reversible transitions of the walker across the sites were transduced by the generation of switchable photocurrents.[24] Also, other DNA machines, such as nucleic acid moving "arms", were constructed on electrodes, and the "mechanical" operations of the systems were followed electrochemically.[25]

A further class of nucleic acid machines involves interlocked DNA rings (e.g., catenanes or rotaxanes).[26,27] Specifically, our laboratory has introduced catenated, interlocked DNA rings that undergo programmed fuel-driven transitions.[26] This is exemplified in Figure 4A by the synthesis of the three-ring linear catenane L. The linear structure L consists of three rings, α, β, and γ. Ring α includes two identical sequence-specific sites I and II complementary to sequence III associated with ring γ. In the presence of the fuel strand (Fu), ring γ is displaced and is translocated across the upper or lower rim of ring β to

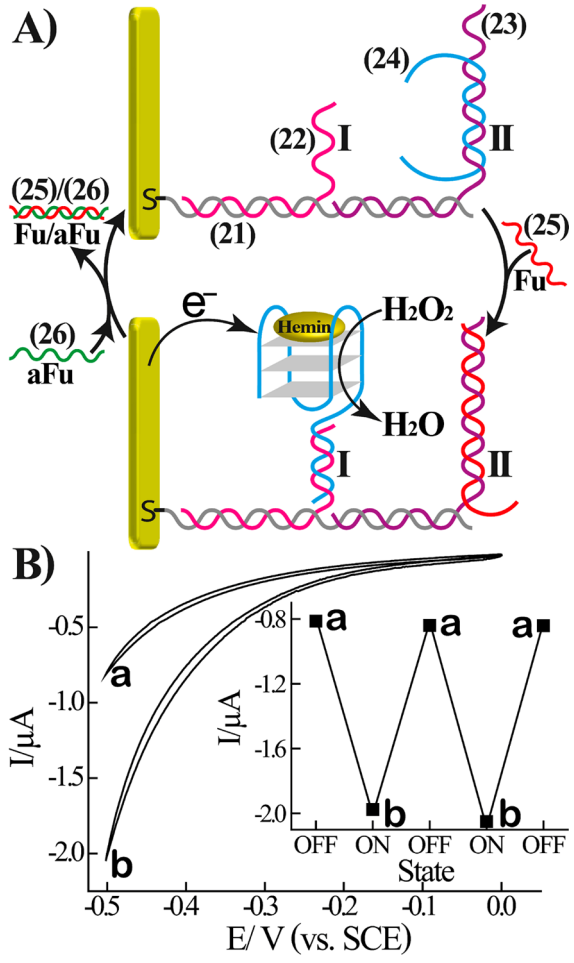

Figure 3. (A) Electrochemical transduction of the cyclic switchable transitions of a nucleic acid "walker" associated with an electrode. (B) Cyclic voltammograms corresponding to (a) the walker positioned on foothold II and (b) the walker positioned on foothold I, accompanied by the self-assembly of the hemin/G-quadruplex structure. The inset shows cyclic amperometric responses of the device when the walker is positioned on (a) foothold II and (b) foothold I. Reprinted with permission from ref 24. Copyright 2013 American Chemical Society.

accommodate sites I or II, yielding the isoenergetic structures P_1 and P_2, respectively. Removal of the fuel strand by the

dx.doi.org/10.1021/ar400316h | Acc. Chem. Res. 2014, 47, 1673−1680

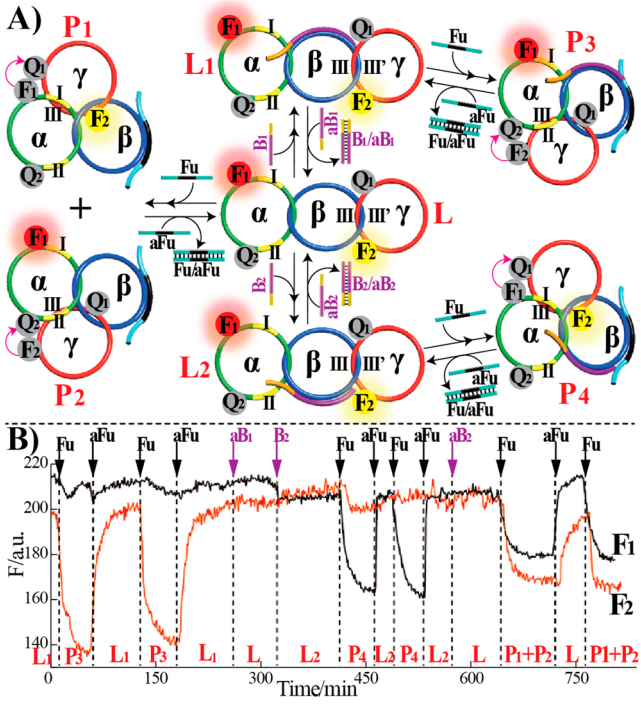

Figure 4. (A) Cyclic reconfiguration of the linear three-ring catenane L: (i) Formation of the structures P_1 and P_2 upon treatment of the linear structure L with the fuel strand (Fu), and the reverse antifuel (aFu)-driven process. (ii) Formation of structure P_3 by blocking of the upper rim of ring β by blocker B_1 and the fueled transition of ring γ to site II of ring α, and the reverse antifuel (aFu)/antiblocker (aB_1)-driven process. (iii) Formation of structure P_4 by blocking of the lower rim of ring β by blocker B_2 and the fueled translocation of ring γ to site I of ring α, and the reverse process in the presence of the antiblocker (aB_2) and antifuel. (B) Time-dependent fluorescence changes upon the cyclic reconfiguration of the three-ring catenane across the states L, P_1/P_2, P_3, and P_4. The rings are labeled with the fluorophores F_1 and F_2 and the quenchers Q_1 and Q_2 to follow the dynamic reconfiguration of the states. Reprinted with permission from ref 26. Copyright 2012 Wiley-VCH.

antifuel strand (aFu) regenerates the energetically stabilized linear structure L. When the upper rim of ring β is blocked with the blocker B_1, treatment of the structure with the fuel strand dictates the directional translocation of ring γ along the lower rim of ring β to selectively occupy site II of ring α, forming structure P_3. Similarly, when the lower rim of ring β in the linear structure L is blocked, the fuel strand stimulates the selective translocation of ring γ to site I of ring α along the upper rim of ring β, forming the structure P_4. By the use of the antifuel strand and the respective antiblocker strands, the structures P_3 and P_4 can be reconfigurated to the linear structure L. Labeling of the three-ring catenane with the two fluorophores F_1 and F_2 and the two quencher units Q_1 and Q_2 allowed the transitions across the different configurations to be followed by fluorescence spectroscopy (Figure 4B).

The concept of fueled dynamic transitions of interlocked, catenated DNA rings was further developed by designing a two-ring catenated rotor system that undergoes dictated clockwise or counterclockwise rotations across three states, using Hg^{2+}/cysteine and/or pH (H^+/OH^-) as fuels/antifuels.[28] Also, by the design of a two-ring interlocked catenane in which ring α includes two binding sites I and II for ring β, the autonomous pH-stimulated activation of a pendulum DNA device wasdemonstrated (Figure 5A).[29] At neutral pH, site II is partially blocked with cytosine-rich strand (**27**). In the blocked

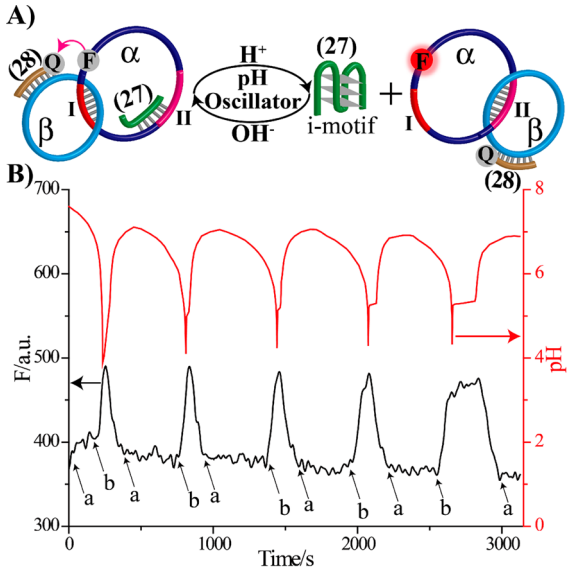

Figure 5. (A) pH activation of a DNA pendulum device consisting of two interlocked rings. (B) Switchable pH changes stimulated by the oscillatory pH system (top) and fluorescence responses upon the pH-stimulated oscillatory changes in the system (bottom). High fluorescence intensities are observed when ring β is positioned on site II (pH 5.2). Reprinted with permission from ref 29. Copyright 2013 American Chemical Society.

structure, ring β hybridizes with the energetically less stable site I. Subjecting the system to an acidic pH stabilizes the blocker in the i-motif structure, resulting in its release from the device. This results in the transition of ring β to site II, where the formation of the energetically stabilized duplex is favored. Subsequent neutralization of the system leads to dissociation of the i-motif, rehybridization of the blocker strand with site II, and displacement of ring β to site I. Labeling of ring α with an internal fluorophore and ring β with a quencher unit, (**28**), allowed the reversible, pH-stimulated transitions of rings α and β between states II and I to be optically imaged. The introduction of the two-ring DNA catenane into a chemical environment that stimulated oscillatory pH changes between acidic and neutral values (a Landolt-type oscillatory pH system)[30] allowed the autonomous pH-stimulated activation of a DNA "pendulum" device (Figure 5B).

SWITCHABLE FLUORESCENCE PROPERTIES OF FLUOROPHORE/AU NANOPARTICLE-MODIFIED DNA MACHINES

The interactions of fluorophores with plasmonic metal nanoparticles (NPs) strongly depend on the spatial separation between the components. While short distances between the fluorophore and the metal NP usually lead to quenching of the fluorescence of the fluorophore, positioning the fluorophore in the plasmonic field of the NP may lead to surface-enhanced fluorescence that is controlled by several parameters, such as the size of the NP, the quantum efficiency of the fluorophore, the refractive index of the medium, and the distance separating the fluorophore and the NP.[31] The dynamic and reversible fuel-driven supramolecular structures of DNA machines were implemented to assemble fluorophore/AuNP-modified DNA

dx.doi.org/10.1021/ar400316h | Acc. Chem. Res. 2014, 47, 1673−1680

machines exhibiting programmed switchable transitions between fluorescence quenching and surface-enhanced fluorescence functions. This is exemplified by the assembly of two tweezers, T_1 and T_2, that were modified on one arm with a 10 nm-sized AuNP and functionalized with a fluorophore at different positions on the counter arm (Figure 6A,B, panels I).[32] The open tweezers T_1 were composed of the arms (**29**) and (**30**) bridged by (**31**), whereas the open tweezers T_2 were composed of arms (**29**) and (**32**) bridged by (**31**). The two open tweezers T_1 and T_2 were closed by the fuel strand (**33**) and reopened by the antifuel strand (**34**), which yielded the duplex (**33**)/(**34**) as waste. By reversible addition of the fuel and antifuel strands, the cyclic closure and opening of the tweezers was achieved. Figure 6A,B, panels II, shows the switchable fluorescence intensities of the fluorophore (Cy3 = indocarbocyanine) upon the cyclic closure/opening of T_1 and T_2 by fuel/antifuel strands. The fluorescence signals generated by the open states represent the reference fluorescence values of the spatially separated fluorophore/AuNP structures. Closure of tweezers T_1 leads to the quenching of the fluorophore, whereas closure of tweezers T_2 results in enhanced fluorescence, although the distance separating the fluorophore and the AuNP is shortened. The dynamic switchable fluorescence functions of the systems, particularly the enhanced fluorescence observed upon closure of tweezers T_2, upon the shortening of the fluorophore/AuNP distance, were theoretically simulated. Figure 6A,B, panels III, shows the theoretically calculated distance-dependent fluorescence intensities of the fluorophores associated with tweezers T_1 and T_2. The geometrically estimated distances separating the fluorophore and the AuNP in the open and closed states of tweezers T_1 and T_2 were then used to evaluate the expected fluorescence intensities. The distances separating the fluorophore and the AuNP in the open T_1 and T_2 states suggest distance-insensitive fluorescence yields of the fluorophore. In turn, the distances separating the fluorophore and AuNP in the closed states of tweezers T_1 and T_2 (ca. 2 and 4 nm, respectively) imply fluorescence quenching and surface-enhanced fluorescence (ca. 12−18%), respectively, consistent with the experimental results.

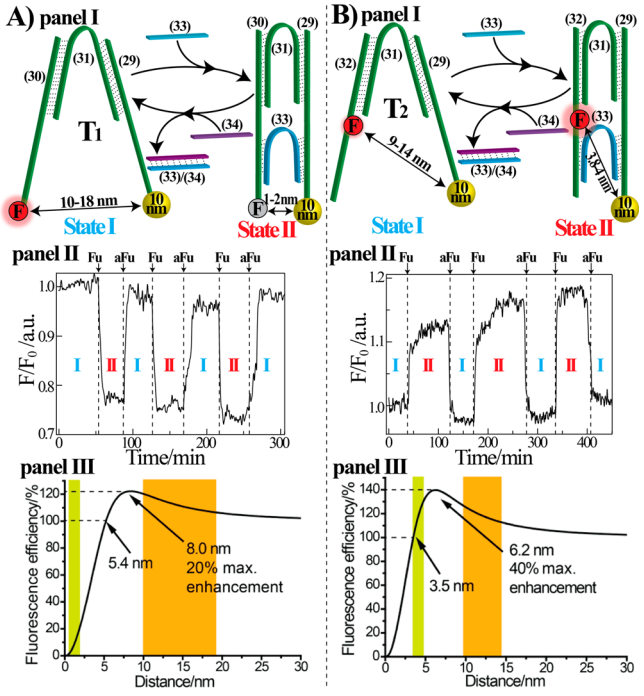

Figure 6. Control of the fluorescence properties of fluorophore/10 nm AuNP conjugates upon the cyclic opening and closure of (A) tweezers T_1 and (B) tweezers T_2 using fuel and antifuel strands. Panels I: Structures of T_1 and T_2. Panels II: Cyclic fluorescence changes upon the closure and opening of the respective tweezers. Panels III: Calculated distance-dependent fluorescence intensities of the Cy3/AuNP conjugates. Bars indicate the geometrically estimated distances separating the fluorophore and AuNP in the closed and open states of the tweezers. Reprinted with permission from ref 32. Copyright 2013 American Chemical Society.

A further interlocked circular fluorophore/AuNP DNA nanostructure that revealed switchable dynamic fluorescence properties is depicted in Figure 7. The system was composed of a DNA ring (**35**) interlocked on a nucleic acid axle (**36**) and stoppered by two 10 nm AuNPs, yielding a rotaxane structure.[33] The sequence I′ associated with ring (**35**) is hybridized with site I of the axle. Site II associated with the axle is also partially complementary to sequence I′, and the site II is blocked by the nucleic acid strand Fu1. The axle of the device is blocked by strands B1 and B2 to introduce rigidity into the axle structure. The interlocked ring was further functionalized with the fluorophore-modified nucleic acids (**37**) and (**38**) that hybridize with the ring sequences X′ and X″, yielding the

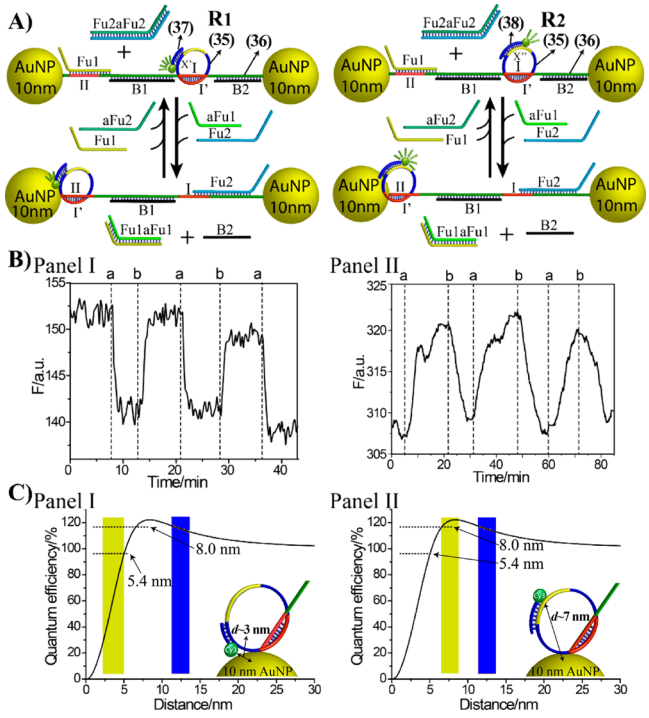

Figure 7. Cyclic control of the fluorescence properties of two fluorophore-functionalized rotaxane devices stoppered by AuNPs undergoing switchable transitions between sites I and II using fuel and antifuel strands. (A) Structures and cyclic transitions of rotaxanes R_1 and R_2. (B) Cyclic fluorescence changes upon the cyclic transitions of the fluorophore-modified rotaxanes between sites I and II. Panel I: rotaxane R_1. Panel II: rotaxane R_2. (C) Calculated distance-dependent fluorescence intensities of the Cy3/10 nm AuNP conjugates. Bars indicate the geometrically estimated distances separating the fluorophore and AuNP in the respective rotaxane structures (blue, ring in site I; orange, ring in site II). Reprinted with permission from ref 33. Copyright 2013 American Chemical Society.

dx.doi.org/10.1021/ar400316h | Acc. Chem. Res. 2014, 47, 1673−1680

nanostructures R_1 and R_2, respectively [the fluorophore Cy3 was attached to the 3′- and 5′-ends of (**37**) and (**38**), respectively] (Figure 7A). Subjecting the molecular devices R_1 and R_2 to the fuel strand Fu2 and the antiblocker strand aFu1 stimulates the transitions of the rings to site II associated with the axle, where the fluorophore retains closer spatial proximity to the AuNP. Subsequent removal of the Fu2 by the antifuel strand aFu2 and further blocking of site II with the blocker unit Fu1 restores the original sites of the rotaxanes, where the rings rest on site I. Panels I and II in Figure 7B show the cyclic switchable fluorescence properties of the devices R_1 and R_2 upon the fuel-driven transitions of the modified rings between sites I and II. For device R_1, switching the fluorophore-functionalized ring to site II leads to fluorescence quenching, while for device R_2, the transition of the fluorophore-functionalized ring to site II results in surface-enhanced fluorescence. These results are consistent with the theoretical simulations of the distance-dependent fluorescence properties of the Cy3/10 nm AuNP systems (Figure 7C). The geometrically estimated distances separating the fluorophores positioned at site I of devices R_1 and R_2 indicate that they exist within the distance-insensitive fluorescence quantum yield domain. The transition of the ring in structure R_1 to site II yields a fluorophore/AuNP separation distance of ca. 3 nm, whereas the translocation of the ring to site II in structure R_2 yields a separation distance of ca. 7 nm, suggesting fluorescence quenching and surface-enhanced fluorescence for devices R_1 and R_2, respectively, as observed experimentally.

PROGRAMMED RECONFIGURATION OF AUNP ASSEMBLIES BY DNA MACHINES

The information encoded in the base sequences of nucleic acids has been used to self-assemble programmed assemblies of metal nanoparticles,[5] such as AuNP tetrahedra, NP wires, and dictated NP structures on DNA origami matrices. Also, ingenious approaches for the construction of three-dimensional crystal-like structures composed of nanoparticles have been reported.[34] The cyclic mechanical stimuli-driven transitions of nucleic acid nanostructures across predesigned states enables the dynamic switchable reconfiguration of programmed metallic NP structures by tethering the NPs to the DNA machines. This is exemplified in Figure 8A by the use of DNA tweezers to reversibly control the structures of AuNPs by the application of single-DNA-modified AuNPs.[32] The (**29**)- and (**39**)-modified 10 nm AuNPs were bridged with the (**40**)-functionalized 5 nm AuNPs to form the open state of the tweezers. In the presence of the fuel strand, (**33**), the bridging of the arms leads to the closed state of the tweezers. The introduction of the antifuel strand, (**34**), regenerates the open state of the tweezers. Figure 8B,C shows scanning transmission electron microscopy (STEM) images of the resulting NP structures. While the open tweezers show spatially separated 10 nm NPs with the 5 nm NP positioned between the larger particles, the closed tweezers reveal a compact structure of the three-NP system.

Similarly, the dynamic transitions of an interlocked three-ring catenane were used to control the reconfiguration of different-sized AuNPs (Figure 9A).[35] The linear three-ring catenane L_1 was modified with two single-DNA-modified 10 nm AuNPs on rings α and γ, and a single-DNA-modified 5 nm AuNP was linked to ring α. As ring α includes two isoenergetic sequences for hybridization of ring γ (domains I and II), controlled dynamic reconfiguration of the three AuNPs structures could be achieved in the presence of the appropriate fuel and blocker

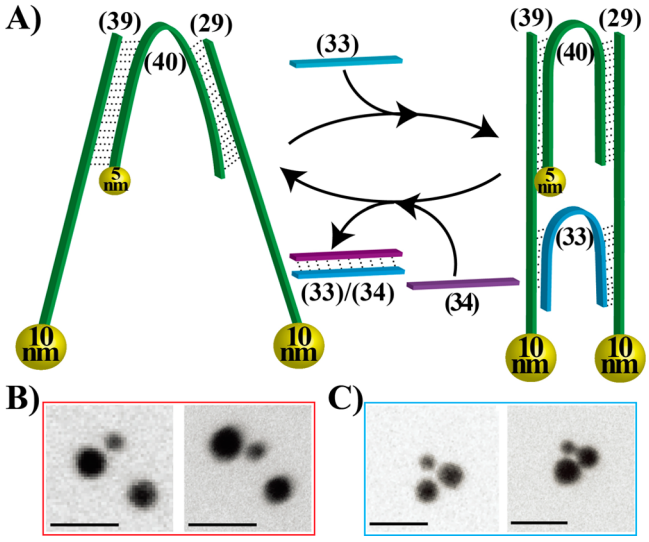

Figure 8. (A) Reconfiguration of AuNP structures by the cyclic opening and closure of a DNA tweezers device. (B, C) STEM images of the three-AuNP structures generated by the open and closed tweezers, respectively. Reprinted with permission from ref 32. Copyright 2013 American Chemical Society.

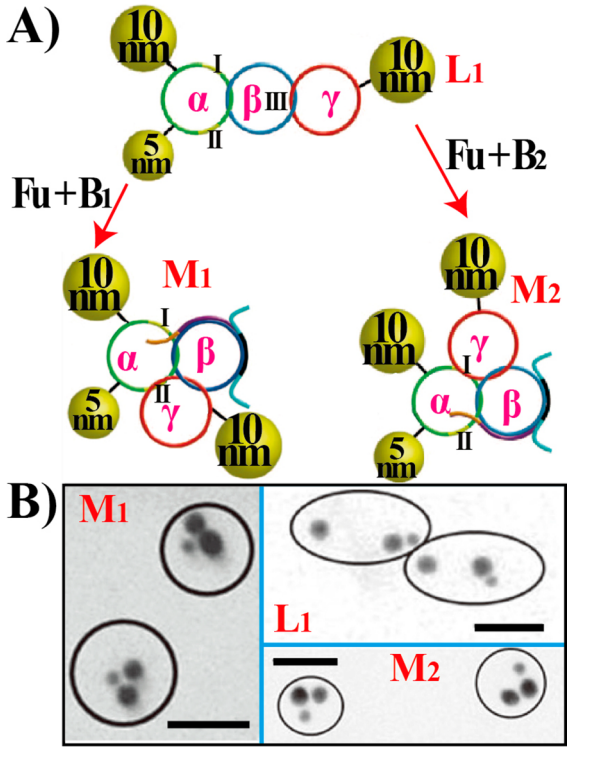

Figure 9. (A) Reconfiguration among the three AuNP structures L_1, M_1, and M_2 by a three-ring catenane device using the respective fuel and blocker strands. (B) STEM images corresponding to the AuNP structures generated by the three-ring catenane device in the configurations L_1, M_1, and M_2. Reprinted with permission from ref 35. Copyright 2013 Nature Publishing Group.

units. Treatment of structure L_1 with the blocker unit B_1 and subsequently with the fuel strand Fu, which displaces ring γ from ring β (site III), results in the transition of ring γ through the lower rim of ring β and the hybridization of ring γ with site II of ring α to yield the NP structure M_1, where the 5 nm AuNP

dx.doi.org/10.1021/ar400316h | Acc. Chem. Res. 2014, 47, 1673−1680

is positioned between the two 10 nm AuNPs. Subjecting the linear structure L_1 to the blocker unit B_2 and subsequently to the fuel strand results in the dynamic transition of ring γ along the upper rim of ring β to hybridize with site I of ring β and reconfigurate the AuNPs into structure M_2, where the 5 nm AuNP is positioned atop two adjacent 10 nm AuNPs. Figure 9B displays STEM images of the AuNP structures generated upon the dynamic reconfiguration of the three-ring catenane system. It should be noted that the reconfiguration of the AuNPs associated with the three-ring catenane system also led to switchable interparticle plasmonic coupling phenomena that were modeled theoretically.[35] However, the plasmonic coupling interactions are relatively weak because of the sizes of the NPs. Similar reconfiguration of AuNPs was demonstrated with a rotaxane structure stoppered by two 10 nm NPs.[33]

■ CONCLUSIONS AND PERSPECTIVES

This Account has introduced several recent advances in the area of DNA machines. One topic that was addressed is the design of machines driven by a sequence of fuels and antifuels. Increasing the types of fuels and antifuels allows the complexity of the DNA machines to be enhanced. For example, the K^+/crown ether cyclic reconfiguration of K^+-stabilized G-quadruplexes was implemented to assemble switchable hydrogels, and by the association and dissociation of hemin to the G-quadruplexes, switchable catalytic hydrogels were constructed.[36] Also, nanoparticle-modified electrodes were used to electrically stimulate pH changes of electrolyte solutions and control the catalytic functions of DNAzymes by an i-motif nanostructure.[37] Thus, the development of new fuels and antifuels and the auxiliary electrochemical generation of triggering stimuli are anticipated to yield new materials and devices that trigger DNA machines.

A further topic that has been addressed in this Account is the development of stimuli-responsive interlocked DNA ring nanostructures (e.g., catenanes and rotaxanes) that undergo programmed transitions across predefined states in the presence of appropriate fuels and antifuels. A three-ring catenane system undergoing dictated transitions across three states was described. Nonetheless, by increasing in the number of interlocked rings (e.g., to five or seven rings), transitions across higher numbers of states may be envisaged. The transitions of molecular devices across higher numbers of states might introduce new concepts for the construction of memory devices. The control over the mechanical operation of different states by means of blocker and antiblocker units might provide a general paradigm for programmed gene transport, delivery, and silencing. Furthermore, the sequences encoded in the circular structures might be designed to specifically bind and release low-molecular-weight or protein substrates (e.g., aptamer sequences). As a result, the interlocked DNA devices might act as programmed carriers that enable controlled release of valuable therapeutic substances. In this context, the advantages of interlocked, circular DNA structures should be emphasized. Since the circular structures lack 3′- and 5′-ends, they are anticipated to be resistant to DNA digestion.

Furthermore, we have emphasized the use of DNA machines as molecular devices to control switchable distance-dependent plasmonic functions and to generate programmed switchable structures of AuNPs. Such systems may provide a rich arena of supramolecular structures for theoretical modeling and fundamental understanding of plasmonic effects. The switchable reconfiguration of nanoparticles by means of DNA machines might find important future applications. For example, light-induced local heating of cells through irradiation of plasmonic particles was reported as a therapeutic means.[38] Thus, the stimuli-controlled clustering of nanoparticles may suggest new medical treatments. Furthermore, at present we have used AuNPs as payloads carried by the DNA machines. The use of other metal nanoparticles, particularly catalytic NPs, may lead to new mechanically controlled electrocatalytic DNA devices. Furthermore, the incorporation of DNA machines into cells and the use of the molecular devices to probe intracellular processes may be envisaged. Indeed, pH-responsive tweezers systems have been applied to monitor intracellular pH changes.[39]

Although substantial progress in developing stimuli-responsive DNA machines has been demonstrated, important challenges are ahead of us. The increase in the complexity of the systems is accompanied by lower yields of the devices, and hence, the development of new synthetic platforms for the systems and their components is essential. To summarize, the area of DNA machines has demonstrated impressive advances in recent years. However, important challenges still exist, and the topic provides a rich field for interdisciplinary research that integrates chemistry, physics, biology, and materials science.

■ AUTHOR INFORMATION

Corresponding Author

*E-mail: willnea@vms.huji.ac.il. Tel: +972-2-6585272. Fax: +972-2-6527715.

Author Contributions

‡X.L. and C.-H.L. contributed equally.

Notes

The authors declare no competing financial interest.

Biographies

Xiaoqing Liu graduated from Changchun Institute of Applied Chemistry, Chinese Academy of Sciences, in 2008. After a postdoctoral research appointment at Aarhus University, Denmark, she joined the laboratory of Itamar Willner at The Hebrew University of Jerusalem as a postdoctoral fellow. Her research interests include DNA sensors and DNA nanotechnology.

Chun-Hua Lu graduated from the College of Chemistry and Chemical Engineering, Fuzhou University, China, in 2011 and is currently a postdoctoral research fellow at The Hebrew University of Jerusalem. His research interests include DNA nanotechnology and DNA-based hydrogels.

Itamar Willner is a Professor of Chemistry at The Hebrew University of Jerusalem. His research interests include nanobiotechnology, nanotechnology, and molecular and biomolecular electronics and optoelectronics. He holds many awards and honors, including the Israel Prize in Chemistry, the EMET Prize, and the Rothschild Prize. He is a member of the Israel Academy of Sciences, the Leopoldina German National Academy of Sciences, and the European Academy of Sciences and Arts. He has coauthored over 670 research papers and monographs and serves on many journal editorial boards.

■ ACKNOWLEDGMENTS

Our research on DNA nanotechnology is supported by the Israel Science Foundation and by the Volkswagen Foundation, Germany.

REFERENCES

(1) Ellington, A. D.; Szostak, J. W. *In vitro* selection of RNA molecules that bind specific ligands. *Nature* **1990**, *346*, 818−822.
(2) Breaker, R. R.; Joyce, G. F. A. DNA enzyme that cleaves RNA. *Chem. Biol.* **1994**, *1*, 223−229.
(3) (a) Seeman, N. C. Nucleic acid junctions and lattices. *J. Theor. Biol.* **1982**, *99*, 237−247. (b) Teller, C.; Willner, I. Organizing protein−DNA hybrids as nanostructures with programmed functionalities. *Trends Biotechnol.* **2010**, *28*, 619−628.
(4) (a) Lin, C.; Liu, Y.; Yan, H. Designer DNA nanoarchitectures. *Biochemistry* **2009**, *48*, 1663−1674. (b) Zheng, J.; Birktoft, J. J.; Chen, Y.; Wang, T.; Sha, R.; Constantinou, P. E.; Ginell, S.; Mao, C.; Seeman, N. C. From molecular to macroscopic via the rational design of a self-assembled 3D DNA crystal. *Nature* **2009**, *46*, 74−77.
(5) Wilner, O. I.; Willner, I. Functionalized DNA nanostructures. *Chem. Rev.* **2012**, *112*, 2528−2556.
(6) Wilner, O. I.; Weizmann, Y.; Gill, R.; Lioubashevski, O.; Freeman, R.; Willner, I. Enzyme cascades activated on topologically programmed DNA scaffolds. *Nat. Nanotechnol.* **2009**, *4*, 249−254.
(7) Willner, I.; Shlyahovsky, B.; Zayats, M.; Willner, B. DNAzymes for sensing, nanobiotechnology and logic gate applications. *Chem. Soc. Rev.* **2008**, *37*, 1153−1165.
(8) Qian, L.; Winfree, E.; Bruck, J. Neural network computation with DNA strand displacement cascades. *Nature* **2011**, *475*, 368−372.
(9) Keren, K.; Krueger, M.; Gilad, R.; Ben-Yoseph, G.; Sivan, U.; Braun, E. Sequence-specific molecular lithography on single DNA molecules. *Science* **2002**, *297*, 72−75.
(10) Modi, S.; Bhatia, D.; Simmel, F. C.; Krishnan, Y. Structural DNA nanotechnology: From bases to bricks, from structure to function. *J. Phys. Chem. Lett.* **2010**, *1*, 1994−2005.
(11) (a) Bath, J.; Turberfield, A. J. DNA nanomachines. *Nat. Nanotechnol.* **2007**, *2*, 275−284. (b) Krishnan, Y.; Simmel, F. C. Nucleic acid based molecular devices. *Angew Chem., Int. Ed.* **2011**, *50*, 3124−3156.
(12) Zhang, D. Y.; Seelig, G. Dynamic DNA nanotechnology using strand-displacement reactions. *Nat. Chem.* **2011**, *3*, 103−113.
(13) Gehring, K.; Leroy, J. L.; Guéron, M. A tetrameric DNA structure with protonated cytosine-cytosine base pairs. *Nature* **1993**, *363*, 561−565.
(14) (a) Alberti, P.; Mergny, J.-L. DNA duplex−quadruplex exchange as the basis for a nanomolecular machine. *Proc. Natl. Acad. Sci. U.S.A.* **2003**, *100*, 1569−1573. (b) Davis, J. T.; Spada, G. P. Supramolecular architectures generated by self-assembly of guanosine derivatives. *Chem. Soc. Rev.* **2007**, *36*, 296−313.
(15) Miyake, Y.; Togashi, H.; Tashiro, M.; Yamaguchi, H.; Oda, S.; Kudo, M.; Tanaka, Y.; Kondo, Y.; Sawa, R.; Fujimoto, T.; Machinami, T.; Ono, A. Mercury^{II}-mediated formation of thymine−Hg^{II}−thymine base pairs in DNA duplexes. *J. Am. Chem. Soc.* **2006**, *128*, 2172−2173.
(16) (a) Asanuma, H.; Ito, T.; Yoshida, T.; Liang, X.; Komiyama, M. Photoregulation of the formation and dissociation of a DNA duplex by using the cis−trans isomerization of azobenzene. *Angew. Chem., Int. Ed.* **1999**, *38*, 2393−2395. (b) You, M.; Chen, Y.; Zhang, X.; Liu, H.; Wang, R.; Wang, K.; Williams, K. R.; Tan, W. An autonomous and controllable light-driven DNA walking device. *Angew. Chem., Int. Ed.* **2012**, *51*, 2457−2460.
(17) Tian, Y.; Mao, C. Molecular gears: A pair of DNA circles continuously rolls against each other. *J. Am. Chem. Soc.* **2004**, *126*, 11410−11411.
(18) Yurke, B. A.; Turberfield, J.; Mills, A. P., Jr.; Simmel, F. C.; Neumann, J. L. A DNA-fuelled molecular machine made of DNA. *Nature* **2000**, *406*, 605−608.
(19) (a) Yin, P.; Yan, H.; Daniell, X. G.; Turberfield, A. J.; Reif, J. H. A unidirectional DNA walker that moves autonomously along a track. *Angew. Chem., Int. Ed.* **2004**, *43*, 4906−4911. (b) Shin, J. S.; Pierce, N. A. A synthetic DNA walker for molecular transport. *J. Am. Chem. Soc.* **2004**, *126*, 10834−10835.
(20) Liu, D.; Balasubramanian, S. A proton-fuelled DNA nanomachine. *Angew. Chem., Int. Ed.* **2003**, *42*, 5734−5736.
(21) Wang, Z.-G.; Elbaz, J.; Remacle, F.; Levine, R. D.; Willner, I. All-DNA finite-state automata with finite memory. *Proc. Natl. Acad. Sci. U.S.A.* **2010**, *107*, 21996−22001.
(22) Elbaz, J.; Wang, Z.-G.; Orbach, R.; Willner, I. pH-stimulated concurrent mechanical activation of two DNA "tweezers". A "SET−RESET" logic gate system. *Nano Lett.* **2009**, *9*, 4510−4514.
(23) Wang, Z.-G.; Elbaz, J.; Willner, I. DNA machines: Bipedal walker and stepper. *Nano Lett.* **2011**, *11*, 304−309.
(24) Liu, X.; Niazov-Elkan, A.; Wang, F.; Willner, I. Switching photonic and electrochemical functions of a DNAzyme by DNA machines. *Nano Lett.* **2013**, *13*, 219−225.
(25) Pelossof, G.; Tel-Vered, R.; Liu, X.; Willner, I. Switchable mechanical DNA "arms" operating on nucleic acid scaffolds associated with electrodes or semiconductor quantum dots. *Nanoscale* **2013**, *5*, 8977−8981.
(26) Elbaz, J.; Wang, Z.-G.; Wang, F.; Willner, I. Programmed dynamic topologies in DNA catenanes. *Angew. Chem., Int. Ed.* **2012**, *51*, 2349−2353.
(27) Ackermann, D.; Schmidt, T. L.; Hannam, J. S.; Purohit, C. S.; Heckel, A.; Famulok, M. A double-stranded DNA rotaxane. *Nat. Nanotechnol.* **2010**, *5*, 436−442.
(28) Lu, C. H.; Cecconello, A.; Elbaz, J.; Credi, A.; Willner, I. A three-station DNA catenane rotary motor with controlled directionality. *Nano Lett.* **2013**, *13*, 2303−2308.
(29) Qi, X. J.; Lu, C. H.; Liu, X.; Shimron, S.; Yang, H. H.; Willner, I. Autonomous control of interfacial electron transfer and the activation of DNA machines by an oscillatory pH system. *Nano Lett.* **2013**, *13*, 4920−4924.
(30) Edblom, E. C.; Orban, M.; Epstein, I. R. J. A new iodate oscillator: The Landolt reaction with ferrocyanide in a CSTR. *J. Am. Chem. Soc.* **1986**, *108*, 2826−2830.
(31) Mertens, H.; Koenderink, A. F.; Polman, A. Plasmon-enhanced luminescence near noble-metal nanospheres: Comparison of exact theory and an improved Gersten and Nitzan model. *Phys. Rev. B* **2007**, *76*, No. 115123.
(32) Shimron, S.; Cecconello, A.; Lu, C. H.; Willner, I. Metal nanoparticle-functionalized DNA tweezers: From mechanically programmed nanostructures to switchable fluorescence properties. *Nano Lett.* **2013**, *13*, 3791−3795.
(33) Cecconello, A.; Lu, C. H.; Elbaz, J.; Willner, I. Au nanoparticle/DNA rotaxane hybrid nanostructures exhibiting switchable fluorescence properties. *Nano Lett.* **2013**, *13*, 6275−6280.
(34) Macfarlane, R. J.; Lee, B.; Jones, M. R.; Harris, N.; Schatz, G. C.; Mirkin, C. A. Nanoparticle superlattice engineering with DNA. *Science* **2011**, *334*, 204−208.
(35) Elbaz, J.; Cecconello, A.; Fan, Z.; Govorov, A. O.; Willner, I. Powering the programmed nanostructure and function of gold nanoparticles with catenated DNA machines. *Nat. Commun.* **2013**, *4*, 2000.
(36) Lu, C. H.; Qi, X. J.; Orbach, R.; Yang, H. H.; Mironi-Harpaz, I.; Seliktar, D.; Willner, I. Switchable catalytic acrylamide hydrogels cross-linked by hemin/G-quadruplexes. *Nano Lett.* **2013**, *13*, 1298−1302.
(37) Frasconi, M.; Tel-Vered, R.; Elbaz, J.; Willner, I. Electrochemically stimulated pH changes: A route to control chemical reactivity. *J. Am. Chem. Soc.* **2010**, *132*, 2029−2036.
(38) Lal, S.; Clare, S. E.; Halas, N. J. Nanoshell-enabled photothermal cancer therapy: Impending clinical impact. *Acc. Chem. Res.* **2008**, *41*, 1842−1851.
(39) Modi, S.; M. G., S.; Goswami, D.; Gupta, G. D.; Mayor, S.; Krishnan, Y. A DNA nanomachine that maps spatial and temporal pH changes inside living cells. *Nat. Nanotechnol.* **2009**, *4*, 325−330.